Quantum transport and stochastic magnetization dynamics simulation on intrinsic spin torque switching asymmetry

Xiaobin Wang, Wenzhong Zhu, and Dimitar Dimitrov
Seagate Technology, 7801 Computer Avenue South, Bloomington, Minnesota 55435, USA

(Received 21 August 2008; revised manuscript received 27 January 2009; published 9 March 2009)

We report on the intrinsic spin torque-induced magnetization switching asymmetry due to the asymmetry in the quantum ballistic spin transport through a magnetic tunneling junction. Magnetization switching behaviors between high and low resistance states are explored using a combined microscopic quantum ballistic spin transport and macroscopic stochastic magnetization dynamics simulation. This model predicts both a higher switching voltage and a steeper slope of voltage versus pulse duration when switching from the parallel state to the antiparallel state, a result consistent with experimental observations.

DOI: 10.1103/PhysRevB.79.104408 PACS number(s): 85.75.−d, 75.60.Jk

I. INTRODUCTION

Spin torque-induced magnetization switching[1,2] in a magnetic tunneling junction (MJT) has received increased attention[3] as a promising method for the writing of magnetic random access memory.[4] In a magnetic tunneling junction, a current is passed through two ferromagnetic thin films: one pinned magnetically and one free, separated by a thin insulating layer. The current is polarized by the pinned reference layer magnetization and switches the magnetization of the free layer. When current passes from the free layer to the reference layer, the magnetization in the free layer is switched to a state parallel to the magnetization of the reference layer. When current passes in the opposite direction, the magnetization is switched to an antiparallel state. The parallel and antiparallel magnetization states correspond to low and high resistance states.

To make a practical storage device, it is not sufficient to understand just the requirements for a fast switching time during a write and acceptable thermal stability during a read. One must also study the origin of observed asymmetries of magnetic switching between the two resistance states. Previously we have studied both the averaged magnetization switching and the switching variations in the nanosecond to second range based upon the stochastic Landau-Lifshitz-Gilbert (LLG) equation with a phenomenological spin torque term.[6,7] In this paper we investigate the intrinsic spin torque-induced magnetization switching asymmetry between the high and low resistance states due to asymmetric ballistic spin transport across the magnetic tunneling junction for voltages biased in different directions. In order to explicitly consider spin torque's dependence upon biasing voltage, we expand the previous model to include the microscopic ballistic quantum spin tunneling process. The combined microscopic ballistic quantum spin transport model and macroscopic stochastic magnetization dynamics model provides the capability to explore the dependence of magnetization switching behavior upon microscopic material.

Section II describes the combined model of microscopic quantum spin transport and macroscopic stochastic magnetization dynamics. Model predictions on intrinsic spin torque switching asymmetry are given in Sec. III and compared to experimental observations.

II. QUANTUM BALLISTIC SPIN TRANSPORT AND STOCHASTIC MAGNETIZATION DYNAMICS MODEL

In order to study the intrinsic magnetization switching asymmetry due to ballistic spin transport across a magnetic tunneling junction, we developed a model combining quantum spin transport with stochastic magnetization dynamics. The quantum spin transport model uses the nonequilibrium Green's function approach with a tight-binding Hamiltonian.[8,9] The Hamiltonian for electrons in the ferromagnetic thin films and the insulating layer is

$$H = \sum_{\sigma,i} (E_b^\sigma + 2t_h^\sigma) c_i^+ c_i - \sum_{\sigma,i} t_h^\sigma c_{i+1}^+ c_i + \text{H.c.}, \quad (1)$$

where E_b^σ and t_h^σ are the band offset and the hopping term, respectively, for the spin channel σ. Following Datta's formalism,[10] the charge density and the spin current-density transport between atomic sites are calculated using the nonequilibrium Green's function:

$$I_{i,i\pm1} = \frac{et}{2\pi\hbar} \int Tr_\sigma [G^<_{i,i\pm1} - G^<_{i\pm1,1}] dE,$$

$$\vec{I}^s_{i,i\pm1} = \frac{t}{4\pi} \int Tr_\sigma [(G^<_{i,i\pm1} - G^<_{i\pm1,1}) \vec{\sigma}] dE, \quad (2)$$

where $\vec{\sigma}$ is the Pauli matrix, $G^<$ is the nonequilibrium Keldysh Green's function, and subscript i refers to the individual atomic site. The detailed technique for calculating the nonequilibrium Green's function can be found in Refs. 10 and 11. In this formalism, the system is partitioned into a channel of tunneling electrons and contacts of ferromagnets. Contacts of ferromagnetic thin film are included through self-energy matrices describing the interactions between channel and contacts. The nonequilibrium Green's functions can be determined using:

$$G^< = iG_R \Sigma^< G_R^+, \quad (3)$$

where $G_R = [E - H - \Sigma_L - \Sigma_R]^{-1}$ is the system retarded Green's function and $\Sigma^< = f_L(\Sigma_L^+ - \Sigma_L) + f_R(\Sigma_R^+ - \Sigma_R)$ is the nonequilibrium self-energy, with $f_{L(R)}$ as the Fermi-Dirac distribution of the left(right) $[L(R)]$ contacts and Σ_L, Σ_R as the self-energy of the $L(R)$ contacts. The self-energy Σ_L, Σ_R can be obtained

 ©2009 The American Physical Society

from the retarded Green's function of the isolated semi-infinite $L(R)$ contacts and channel-contact coupling strength.

Conservation of the total angular momentum implies that the spin torque current lost at an atomic site i is transferred to its local magnetic moment, thereby exerting a local spin transfer torque on site i: $\vec{T}_i = \vec{I}^s_{i-1,i} - \vec{I}^s_{i,i+1}$. The net spin torque on the magnetization of the ferromagnetic thin film can be obtained from Eq. (2):

$$\vec{T} = \sum_i (\vec{I}^s_{i-1,i} - \vec{I}^s_{i,i+1}) = \vec{I}^s_{-1,0} - \vec{I}^s_{\infty,\infty} = \vec{I}^s_{-1,0}. \quad (4)$$

Here the spin current density is assumed to decay to zero inside the ferromagnetic thin film. Thus the spin torque magnitude does not depend upon the ferromagnetic thin-film thickness but only on the energy-band splitting of the ferromagnetic material. As explained in Ref. 9, Eqs. (2) and (4) give two components of the spin torque transverse to the thin-film magnetization direction. The in-plane component of the torque is parallel to the thin-film plane, and the out-of-plane component of the torque is perpendicular to thin-film plane. The spin current component longitudinal to the magnetization direction vanishes. Spin transfer torque (4) has the unit of energy, (erg). When normalized by the thin-film magnetic element moment $M_s V$ (emu), it has the unit of magnetic field (Oe).

The magnetization dynamics in the free layer of a MTJ stack is described by the stochastic Landau-Lifshitz-Gilbert equation at a finite temperature with spin torque terms:

$$\frac{d\vec{m}}{dt} = -\alpha\vec{m} \times [\vec{m} \times (\vec{h}_{\text{eff}} + \vec{h}_{\text{fluc}})] - \vec{m} \times (\vec{h}_{\text{eff}} + \vec{h}_{\text{fluc}}) + \frac{\vec{T}_{\text{norm}}}{M_s}, \quad (5)$$

where $\vec{m}$ is the normalized magnetization vector, time t is normalized by γM_s with γ being the gyromagnetic ratio, $\vec{h}_{\text{eff}} = \vec{H}_{\text{eff}}/M_s = \frac{\partial \varepsilon}{\partial \vec{m}}$ is the normalized effective magnetic field with normalized energy density ε, and α is the damping parameter. $\vec{h}_{\text{fluc}}$ is the thermal fluctuation field, whose magnitude is determined by the fluctuation-dissipation condition at room temperature and whose formalism follows Ref. 5. $\vec{T}_{\text{norm}} = \frac{\vec{T}}{M_s V}$ is the normalized spin torque term with units of magnetic field. The net spin torque term $\vec{T}$ is simulated by the microscopic quantum transport described in previous paragraphs. The detailed technique of solving Eq. (5) for switching time versus spin torque magnitude can be found in Refs. 6 and 7. The dynamic thermal switching behavior of the magnetic element depends upon the spin torque magnitude, the thin-film element geometry, and its magnetic properties.

Our modeling method can be summarized as follows: first, a nonequilibrium Green's function is obtained from Eq. (3) based upon the Hamiltonian in Eq. (1) for electrons in the ferromagnetic thin films and the insulating layer. Second, the charge current density and spin current density are calculated from Eq. (2) utilizing a nonequilibrium Green's function. Third, spin torque components transverse to the thin-film magnetization are obtained from Eq. (4) based on total angular-momentum conservation. Finally, the mean magnetization reversal time is calculated for the magnetic thin film at room temperature by solving stochastic LLG Eq. (5) with the spin torque term calculated in the previous steps. There are two sets of parameters for this combined microscopic electronic-spin transport model and macroscopic magnetization dynamics model. The microscopic parameters determining the spin torque $\vec{T}$ are: the Fermi energy level, the insulating barrier height and thickness, the band splitting parameter for the spin-up and spin-down channels in the ferromagnetic thin film, and the effective mass for the ferromagnetic thin films and insulator. The hopping rate in Eq. (1) is related to the electron effective mass, m_{eff}, via $t_h = \frac{\hbar^2}{2m_{\text{eff}}a^2}$, where $\hbar$ is the Planck constant and a is the atomic spacing (of 2 Å for this paper). The macroscopic magnetic parameters determining the stochastic magnetization dynamics are: the magnetization saturation, the magnetic element length, width, and thickness, the crystal anisotropy, and the damping parameter. All the simulations are performed at room temperature (300 K).

III. SPIN TORQUE SWITCHING ASYMMETRY IN MAGNETIC TUNNELING JUNCTIONS

The dependence of charge and spin transports on microscopic parameters of ballistic tunneling models has been discussed extensively in various papers. The bias voltage dependence of the tunneling magnetoresistance ratio (TMR) on insulator barrier height, barrier width, and effective electron mass was discussed in Refs. 11 and 12. Reference 8 described the bias voltage dependence of the tunneling current and spin torque on insulator barrier height, barrier width, and effective electron mass. The bias voltage dependence of spin torque on ferromagnetic band splitting was covered in Refs. 9 and 13.

In this section we examine the magnetization switching predicted by our combined microscopic quantum ballistic transport model and macroscopic stochastic magnetization dynamics model. The model microscopic parameters were chosen to give TMR and resistance multiplying surface area (RA) values close to the experimental measurement. TMR is defined as the difference between the maximum and minimum resistances of a device, divided by the minimum resistance. RA is defined as the product of the low resistance (for parallel magnetization configuration) times the MTJ junction surface area. The measured TMR of our device at zero voltage is approximately 120%, and the RA is approximately 10 $\Omega(\mu\text{m})^2$ for 40 mV biasing across the junction.

Figure 1 shows the measured TMR as a function of biasing voltage for one of our magnetic tunnel junction devices. The MTJ devices were prepared on AlTiC substrates using an Anelva magnetron sputtering system. Figure 2(a) shows the modeled current density as a function of biasing voltage for both the parallel (lower resistance) and the antiparallel states (higher resistance). Figure 2(b) shows the modeled TMR roll off as a function of biasing voltage. The model predicts a TMR close to 120% at zero biasing voltage and an RA value of approximately 10 $\Omega(\mu\text{m})^2$ near 40 mV.

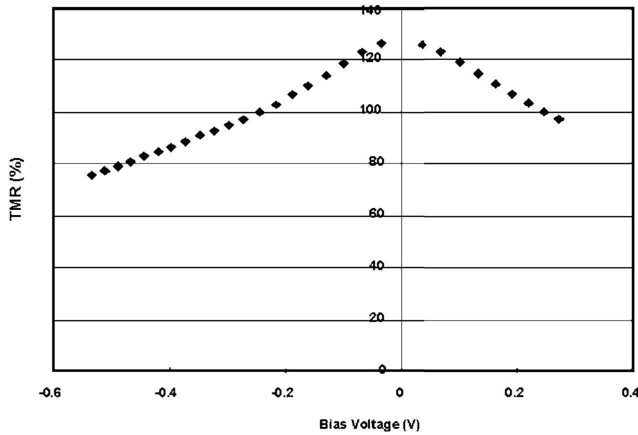

FIG. 1. Experimental measurement of TMR as a function of biasing voltage for a tunneling device of length of 176 nm, width of 100 nm, and thickness of 1.8 nm. TMR is defined as the ratio of (maximum resistance–minimum resistance) divided by minimum resistance.

The microscopic quantum transport model parameters are as follows: the Fermi level is set to zero, and all the other energy-level parameters are relative to the Fermi energy; the insulating barrier is 0.14 eV above the Fermi surface; the bottom energy band for the spin-down channel is 2 eV below the Fermi surface; the band splitting parameter is 1.56 eV; the insulating layer thickness is 8 Å. The effective mass for the ferromagnetic thin film is equal to the free-electron mass, and the effective mass for the insulating barrier is 0.138 times the free-electron mass.

It should be pointed out here that we are not expecting to make an exact match between the measured and simulated biasing voltage dependences of the TMR. The measured dependence of resistance or TMR on biasing voltage involves complex physical processes of inelastic tunneling and asymmetry of the concentration of defects or dopants in the interfacial microstructure.[14] These physical processes are not included in our ballistic transport model, and therefore we do not expect the ballistic model to predict the exact shape of the measured TMR biasing voltage roll off. This is reflected in the differing TMR roll-off slopes between the experimental and the modeled data at small biasing voltages in Figs. 1 and 2(b). Our purpose is to show the intrinsic ballistic spin transport asymmetry effects upon dynamic thermal magnetization switching, using an example set of microscopic parameters giving a TMR and RA prediction close to the measured values. In this case the model predicts a symmetric electronic charge transport between positive and negative voltage biasings. However, the result is very different for the spin torque effects.

Figure 3 shows the modeled voltage bias dependence of both the spin torque in-plane and out-of-plane components for the case of the free layer magnetization oriented at 90° to the reference layer magnetization. The shapes of the simulated voltage dependence of the in-plane and out-of-plane spin torque components are qualitatively in agreement with the measured spin torque torkances,[15] where the torkance is defined as the derivative of the spin torque with respect to voltage. It is clear that the in-plane torque is not symmetric

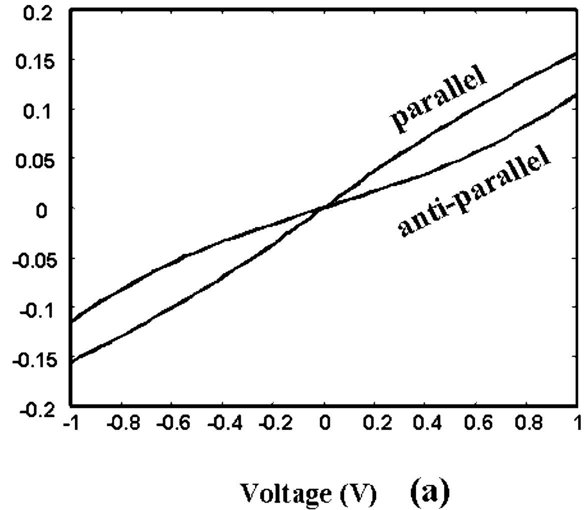

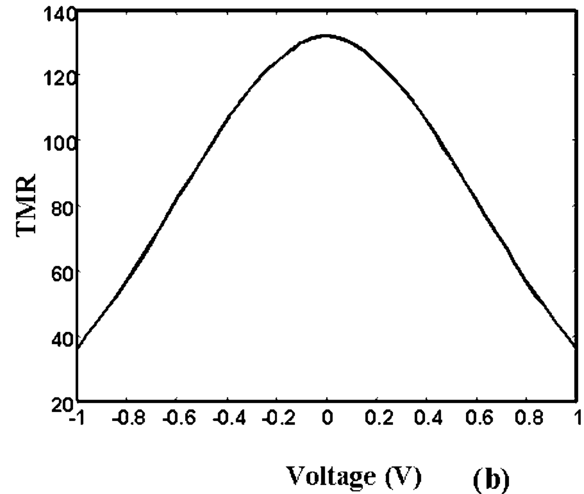

FIG. 2. Simulated current versus biasing voltage, and TMR versus biasing voltage.

between positive and negative bias voltages. In our simulation, the torque for positive voltage corresponds to switching from parallel to antiparallel states (or from low resistance to high resistance), and the torque for negative voltage corresponds to switching in the reverse order.

Figure 3 shows that the modeled out-of-plane torque is symmetric between positive and negative voltage biasings. However, for the case of an out-of-plane spin torque pointing in a fixed direction, the contributions to the magnetization switching from parallel state to antiparallel state and those from antiparallel state to parallel state are exactly opposite. The negative magnitude of the out-of-plane torque in this simulation helps magnetization switching from the antiparallel to the parallel state and inhibits magnetization switching from the parallel to the antiparallel state.

The dynamic thermal magnetization switching biasing voltage as a function of switching time is plotted in Fig. 4. The modeled curves are based on a magnetic element of length 176 of nm, width of 100 nm, and thickness of 1.8 nm. The saturation magnetization is 1000 emu/cc, the crystal anisotropy is 20 Oe, and the damping parameter is 0.0057.

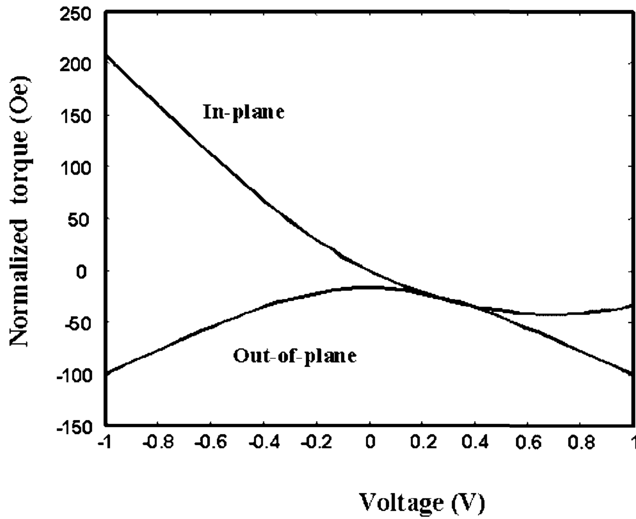

FIG. 3. Simulated voltage bias dependence of normalized spin torque $\vec{T}_{\text{norm}}=\frac{\vec{T}}{M_s V}$ for the case of free layer magnetization oriented at 90° to the reference layer magnetization. The figure shows in-plane and out-of-plane spin torque components.

These parameters were chosen to match the patterned dimensions of the experimental device and the measured magnetic properties of the bulk film. The model predicts that the magnetization switching from the parallel state to the antiparallel state requires a higher voltage than is needed for switching from the parallel state to the antiparallel state. Also the slope of the voltage versus pulsing time is steeper for switching from the parallel state to the antiparallel state. For a 10 ns switching time, the voltage to switch from the parallel state to the antiparallel state is nearly double that which is needed for switching from the antiparallel state to the parallel state.

The experimental measurements for our device are presented as squares in Fig. 4. Our experimental measurements show the same trend of higher voltage and steeper slope of

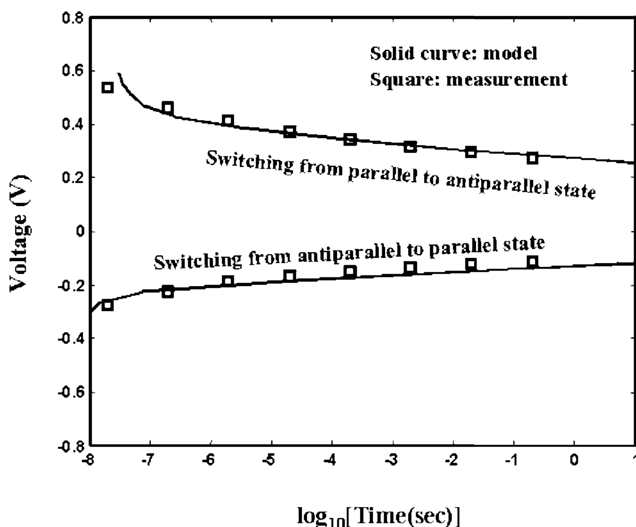

FIG. 4. Theoretical calculation and experimental measurement of switching voltage versus pulse duration time.

voltage versus pulse time for switching from the parallel to antiparallel states. This asymmetric characteristic can be explained by the quantum transport simulation of spin torque illustrated in Fig. 3. At a larger biasing voltage, the simulated in-plane spin torque is smaller in magnitude for the parallel to antiparallel switching case. This means that a higher biasing voltage is needed to switch from the parallel to the antiparallel state, and the corresponding slope of the voltage versus pulse width is steeper. Moreover as mentioned before, the out-of-plane torque helps switching from the antiparallel state to the parallel state and inhibits switching in the opposite direction. Thus both the in-plane and out-of-plane components of the torque contribute to the asymmetric feature of higher voltage and steeper slope for switching from the parallel state to the antiparallel state.

It should be pointed out that there are other sources of switching asymmetry. Examples include both field effects (an unbalanced field of orange-peel coupling and the demagnetization field of the MTJ stack) and the nonuniform current distribution in the high TMR magnetic tunneling junctions. Those contributions can be taken into account by means of micromagnetic simulations.[16] To determine the effects of possible unbalanced fields, we measured the magnetic field-induced free layer magnetization switching of the experimental device. Our measurement showed a centered resistance versus external magnetic field loop. This indicates that our MTJ stack free layer field is balanced. Note that our model is a tight-binding ballistic electronic and spin transport model: it does not include nonuniform current distributions and other inelastic-scattering processes that could contribute to switching asymmetry. The purpose of this study is to show the effects of intrinsic ballistic spin tunneling asymmetry on the dynamic thermal magnetization switching behavior. Using an example set of microscopic and macroscopic parameters, our combined quantum transport and stochastic magnetization dynamics simulation gives TMR, RA, and switching asymmetry results comparable to our device measurements and many published experimental works.[17–20]

Figure 5 shows an example of the measured bias voltage dependence of spin torque switching in MgO based MTJs in a recent experiment by another group.[20] As in our measurement, the magnetic field in their experiment has been balanced. Although the detailed magnetic parameters of the measurements in Ref. 20 are not the same as the theoretical simulation parameters in Fig. 4, their experimental measurement shows the same trends of higher voltage and steeper slope of voltage versus pulse time for parallel state to antiparallel state switching. Similar trends are also observed in earlier measurements, such as in Ref. 19. Again we want to point out that the comparison to experiment here is only for the general trend and magnitude. A direct one-to-one model-to-experiment comparison is not accurate without considering many other tunneling mechanisms that could affect the MTJ electronic and spin transports.

Using the plotted switching voltages and the RA and thin-film device dimensions that were listed earlier, one can infer the measured and modeled critical switching currents. The critical switching current density is defined as the switching voltage divided by RA, and the critical switching current can

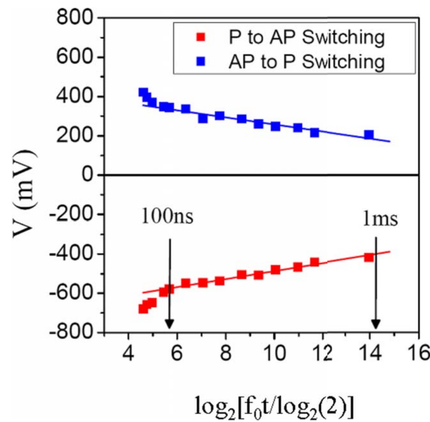

FIG. 5. (Color online) Experimental measurement of switching voltage versus pulse duration time from Ref. 20. The top curve represents switching from the parallel state to the antiparallel state, and the bottom curve represents switching from the antiparallel state to the parallel state.

be calculated by multiplying this critical switching current density by the thin-film surface area.

Note that the spin torque term in Eq. (4) is independent of thin-film thickness due to the assumption that the spin current density decays to zero inside the ferromagnetic thin film. The normalized spin torque term found in stochastic LLG Eq. (5), $\vec{T}_{\text{norm}}=\frac{\vec{T}}{M_s V}$ (in units of magnetic field), is inversely proportional to the film thickness. Thus the critical switching current is roughly proportional to the inverse of the thin-film thickness. For a more realistic dependence of the critical switching current on film thickness, it is necessary to consider the change in demagnetization field when the film thickness is varied, as is done in our model.

IV. CONCLUSIONS

Spin torque-induced magnetization switching asymmetries are studied based on a model combining both microscopic ballistic spin transport and macroscopic stochastic magnetization dynamics. Using a typical set of microscopic and macroscopic parameters, our combined quantum transport and stochastic magnetization dynamics simulation gives TMR, RA, and switching asymmetry results in close agreement to our experimental measurement. The model predicts a higher switching voltage and steeper slope of voltage versus pulse time for the parallel state to antiparallel state switching, which is consistent with our own and other experimental observations.

[1] J. C. Slonczewski, J. Magn. Magn. Mater. **159**, L1 (1996).
[2] L. Berger, Phys. Rev. B **54**, 9353 (1996).
[3] See references cited in J. C. Sankey, Y.-T. Cui, J. Z. Sun, J. C. Slonczewski, R. A. Buhrman, and S. C. Ralph, Nat. Phys. **4**, 67 (2008).
[4] M. Hosomi, H. Yamagishi, H. Ymamoto, T. Bessho, K. Higo, Y. Yamane, K. Yamada, H. Shoji, M. Hachino, H. Fukumoto, C. Nagao, and H. Kano, in *IEEE International Electron Devices Meeting 2005*, 5 December 2005, Washington, DC [IEDM Tech. Digest, 459 (2005)].
[5] W. F. Brown, Jr., Phys. Rev. **130**, 1677 (1963); I. N. Krivorotov, N. C. Emley, A. G. F. Garcia, J. C. Sankey, S. I. Kiselev, D. C. Ralph, and R. A. Buhrman, Phys. Rev. Lett. **93**, 166603 (2004); Z. Li and S. Zhang, Phys. Rev. B **69**, 134416 (2004); D. M. Apalkov and P. B. Visscher, *ibid.* **72**, 180405(R) (2005); J. L. Garcia-Palacios and F. J. Lazaro, *ibid.* **58**, 14937 (1998).
[6] X. Wang, Y. Zheng, H. Xi, and D. Dimitrov, J. Appl. Phys. **103**, 034507 (2008).
[7] X. Wang, W. Zhu, and D. Dimitrov, Phys. Rev. B **78**, 024417 (2008).
[8] S. Salahuddin, D. Datta, P. Srivastava, and S. Datta, in *IEEE International Electron Devices Meeting 2007*, 10 December 2007, Washington, DC, p. 121.
[9] I. Theodonis, N. Kioussis, A. Kalitsov, M. Chshiev, and W. H. Butler, Phys. Rev. Lett. **97**, 237205 (2006).
[10] S. Datta, *Electronic Transport in Mesoscopic Systems* (Cambridge University Press, Cambridge, 1995).
[11] A. A. Yanik, G. Klimeck, and S. Datta, Phys. Rev. B **76**, 045213 (2007).
[12] N. N. Beletskii, G. P. Berman, A. R. Bishop, S. A. Borysenko, and V. M. Yakovenko, Phys. Rev. B **75**, 174418 (2007).
[13] J. Xiao, G. E. W. Bauer, and A. Brataas, Phys. Rev. B **77**, 224419 (2008).
[14] J. C. Slonczewski and J. Z. Sun, J. Magn. Magn. Mater. **310**, 169 (2007).
[15] J. C. Sankey, Y.-T. Cui, J. Z. Sun, J. C. Slonczewski, R. A. Buhrman, and S. C. Ralph, Nat. Phys. **4**, 67 (2008).
[16] K. Lee, A. Deac, O. Redon, and J. Nozieres, Nature Mater. **3**, 877 (2004); B. Montigny and J. Miltat, J. Appl. Phys. **97**, 10C708 (2005); L. Torres, L. Lopez-Diaz, E. Martinez, M. Carpentieri, and G. Finocchio, J. Magn. Magn. Mater. **286**, 381 (2005).
[17] D. D. Djayaprawira, K. Tsunekawa, M. Nagai, H. Maehara, S. Yamagata, N. Watanabe, S. Yuasa, Y. Suzuki, and K. Ando, Appl. Phys. Lett. **86**, 092502 (2005).
[18] A. A. Khan, J. Schmalhorst, A. Thomas, O. Schebaum, and G. Reiss, J. Appl. Phys. **103**, 123705 (2008).
[19] H. Kubota, A. Fukushima, Y. Ootani, S. Yuasa, K. Ando, H. Maehara, K. Tsunekawa, D. D. Djayaprawira, N. Watanabe, and Y. Suzuki, Jpn. J. Appl. Phys., Part 1 **44**, L1237 (2005).
[20] S. C. Oh, K. T. Nam, J. E. Lee, W. J. Kim, J. H. Jeoung, D. K. Kim, S. Y. Lee, K. Kim, U. Chung, and J. T. Moon, in International Conference on Magnetics, May 2008, Spain (unpublished). We thank Oh for sharing his presentation material "Switching characteristics and bias voltage dependence of spin torque switching in MgO based MTJs" with us. Data in Fig. 5 is a copy of his presentation figure.